Indium(III) {2}-Metallacryptates Assembled from 2,6-Dipicolinoyl-bis(*N*,*N*-diethylthiourea)

Chien Thang Pham,[a] *Maximilian Roca Jungfer,*[b] *and Ulrich Abram**[b]

[a] VNU University of Science, Vietnam National University, Hanoi, 19 Le Thanh Tong, Hanoi, Vietnam

[b] Freie Universität Berlin, Institute of Chemistry and Biochemistry, Fabeckstr. 34-36, D-14195 Berlin, Germany

Table of Contents

Part 1 Spectroscopic data

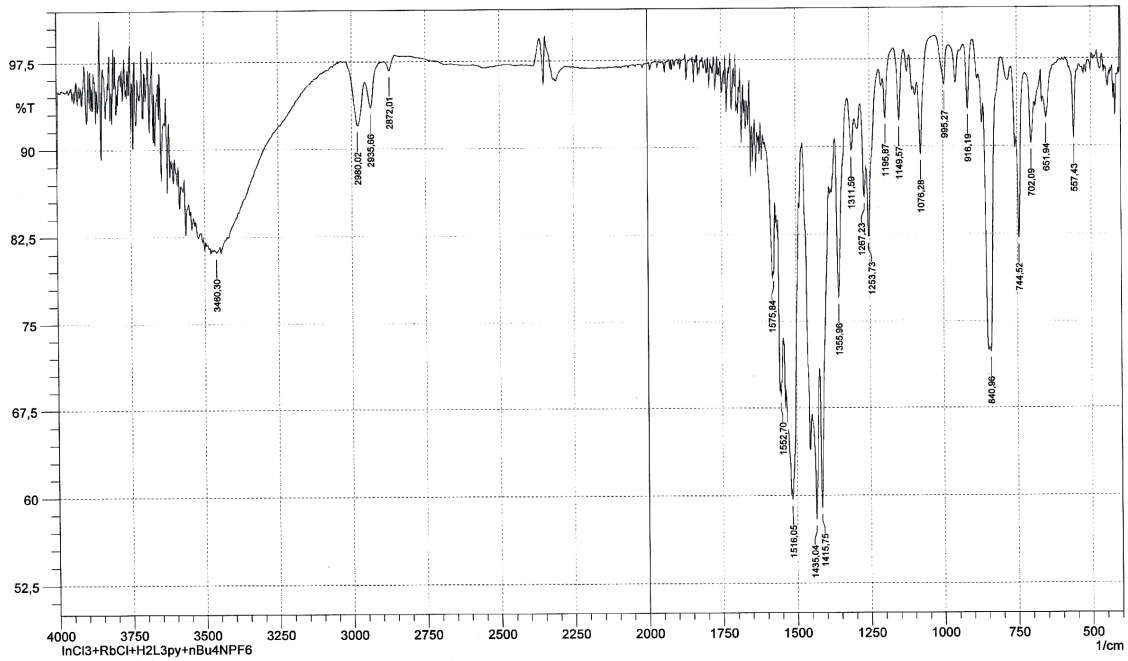

Figure S1.1 IR spectrum of $\{Rb \subset [In_2(L^{py})_3]\}(PF_6)$

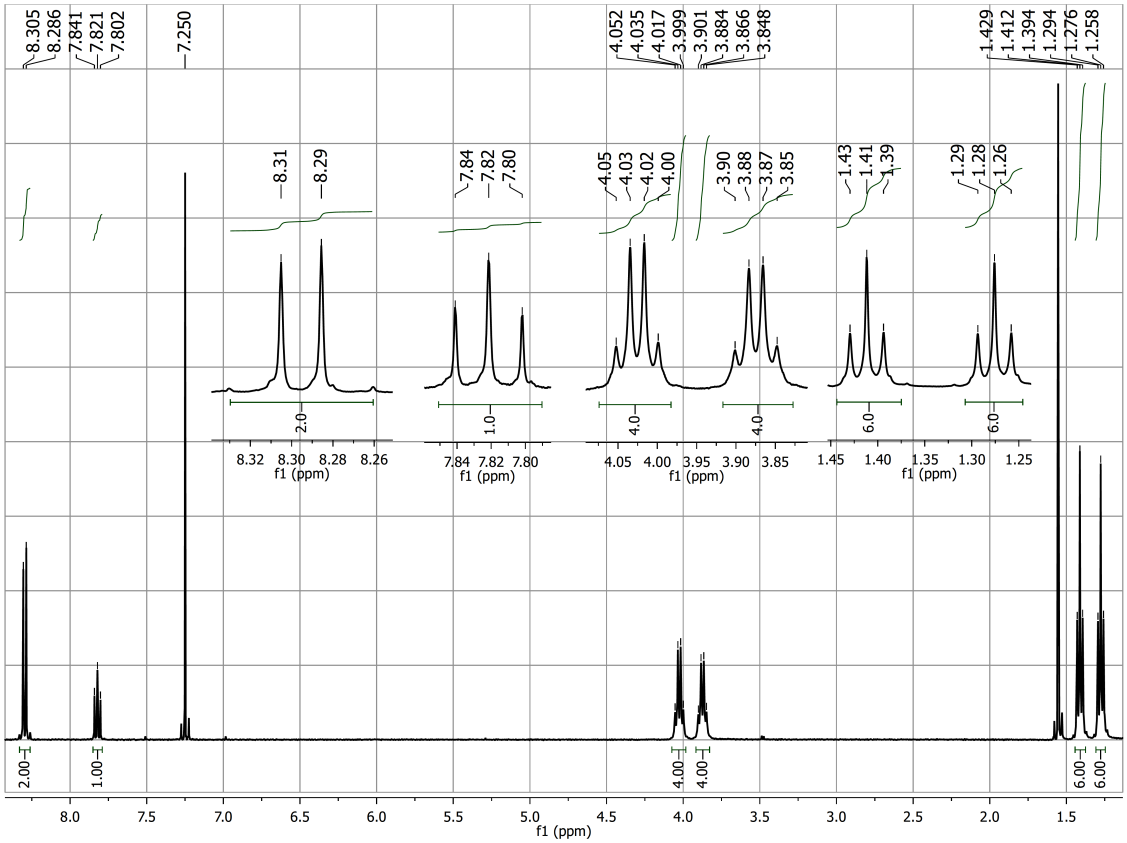

Figure S1.2 ^{1}H NMR spectrum of $\{Rb \subset [In_2(L^{py})_3]\}(PF_6)$ in $CDCl_3$

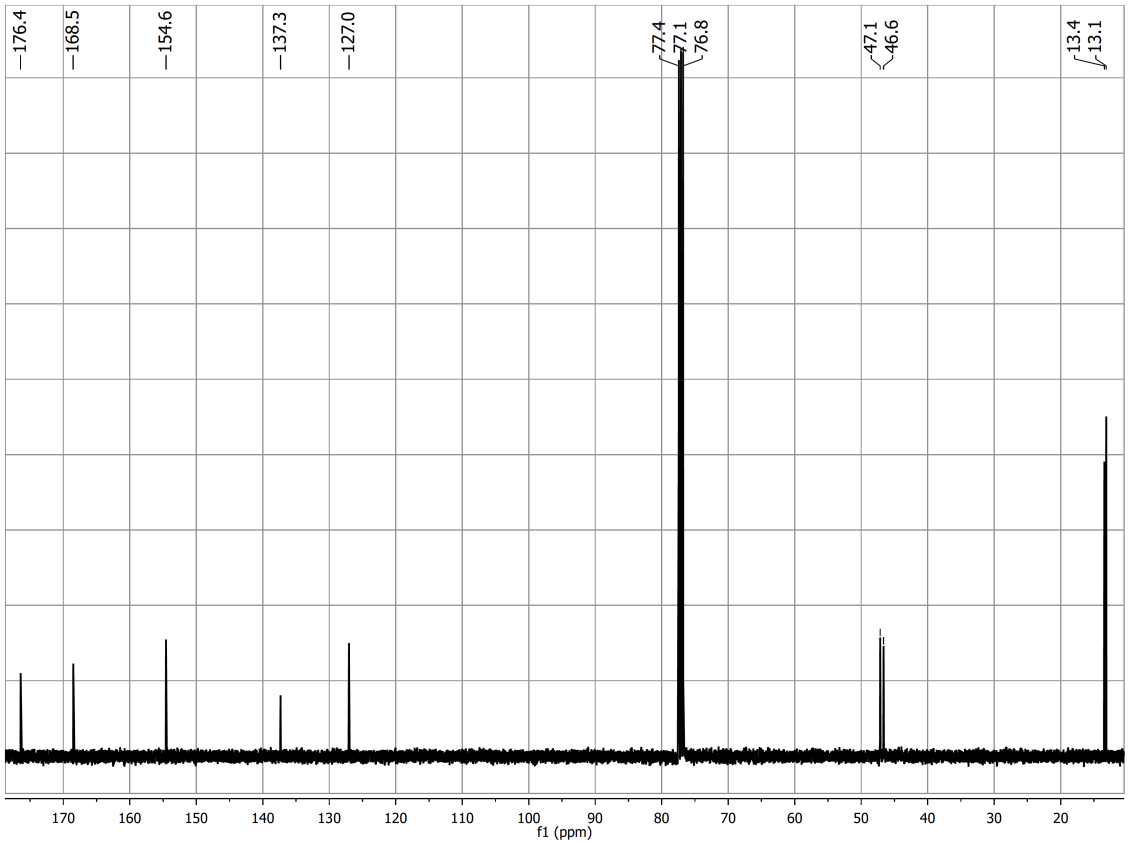

Figure S1.3 $^{13}C\{^{1}H\}$ NMR spectrum of $\{Rb \subset [In_2(L^{py})_3]\}(PF_6)$ in $CDCl_3$

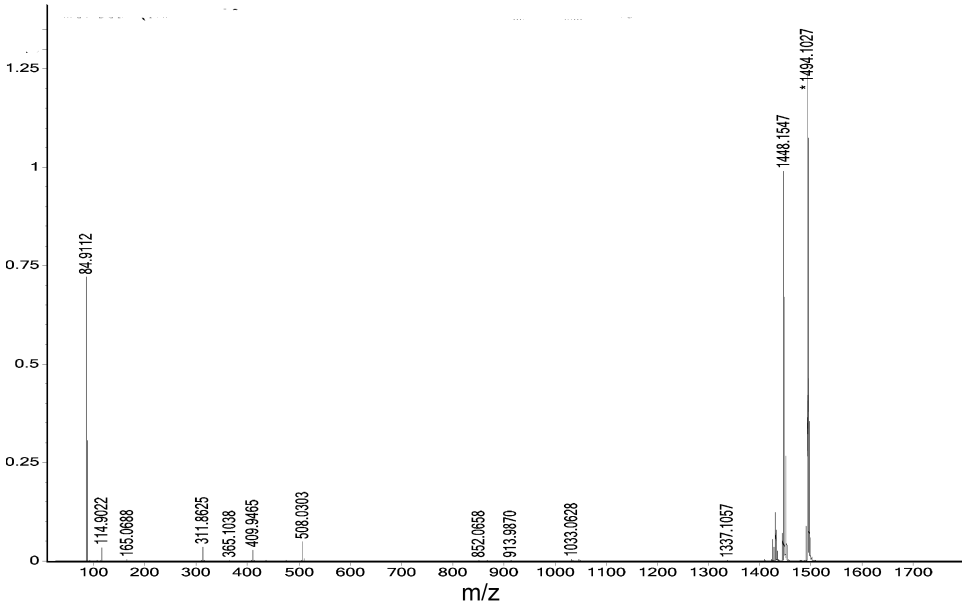

Figure S1.4 High resolution ESI^+ mass spectrum of $\{Rb \subset [In_2(L^{py})_3]\}(PF_6)$. The peaks of the K^+ and Na^+ inclusion compounds are due to interactions with the matrix of the spectrometer, where these ions are present as contaminations.

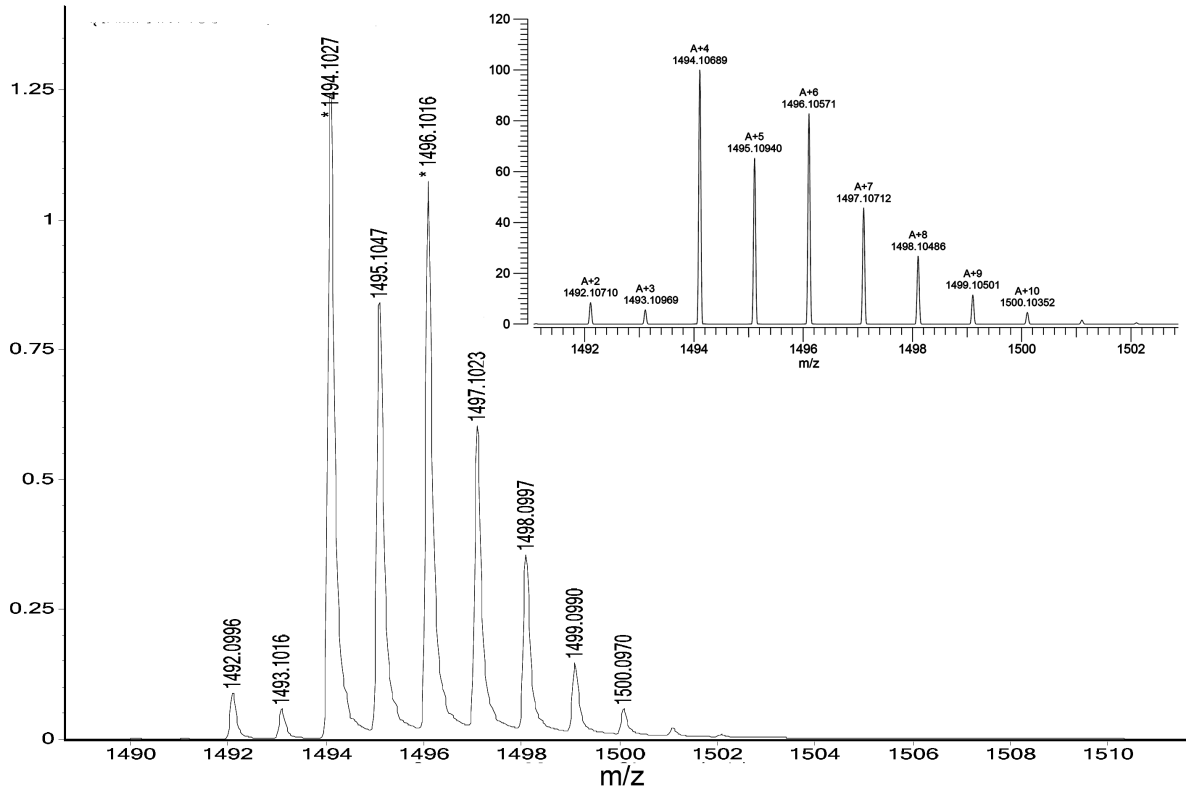

Figure S1.5 Observed and simulated patterns of the based peak in ESI$^+$ mass spectrum of $\{Rb \subset [In_2(L^{py})_3]\}(PF_6)$

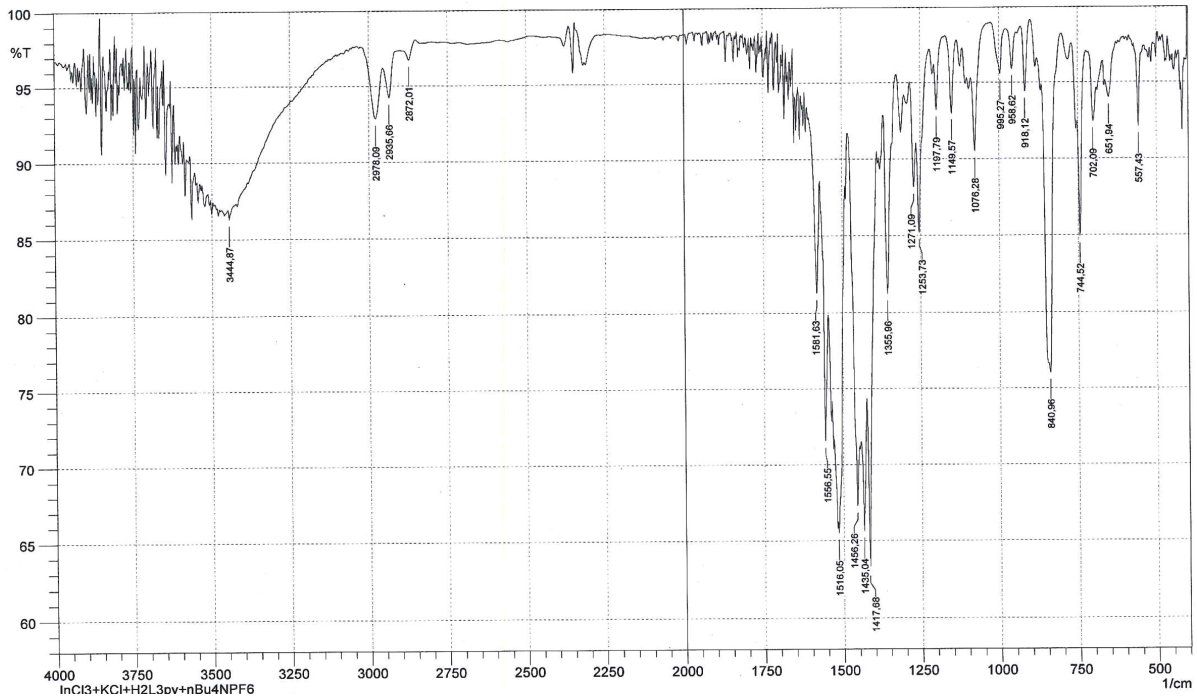

Figure S1.6 IR spectrum of $\{K \subset [In_2(L^{py})_3]\}(PF_6)$

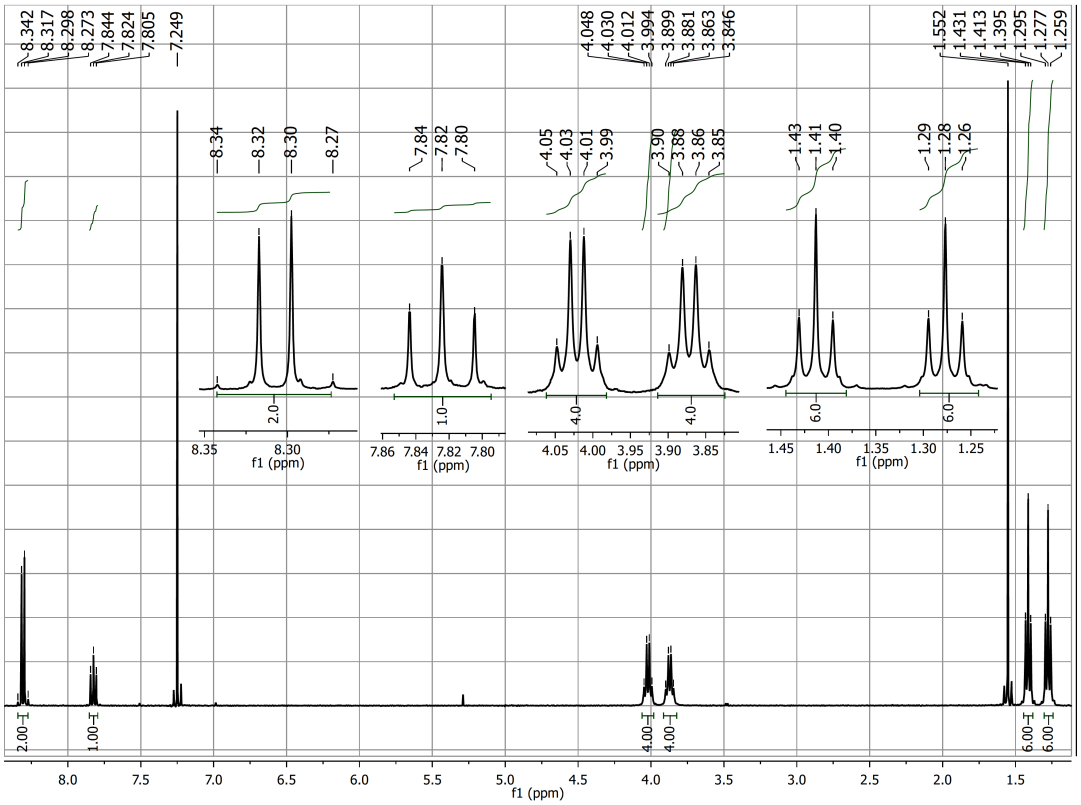

Figure S1.7 ^{1}H NMR spectrum of $\{K \subset [In_2(L^{py})_3]\}(PF_6)$ in $CDCl_3$

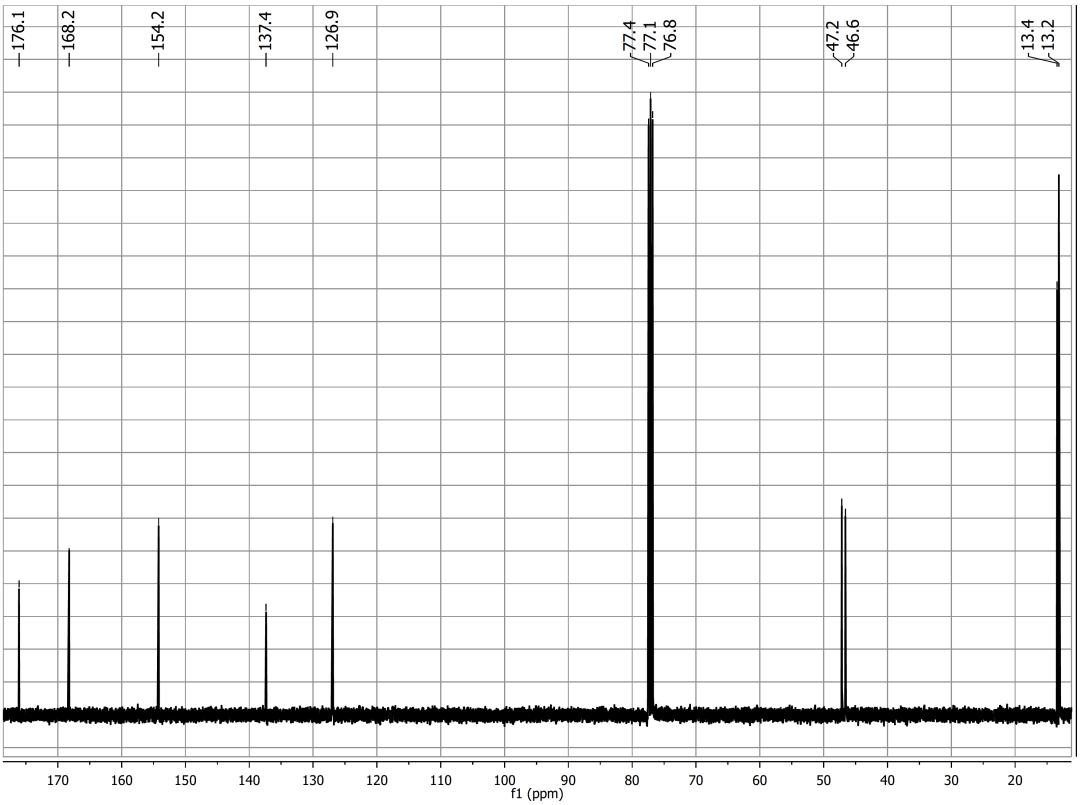

Figure S1.8 ^{13}C{^{1}H} NMR spectrum of $\{K \subset [In_2(L^{py})_3]\}(PF_6)$ in $CDCl_3$

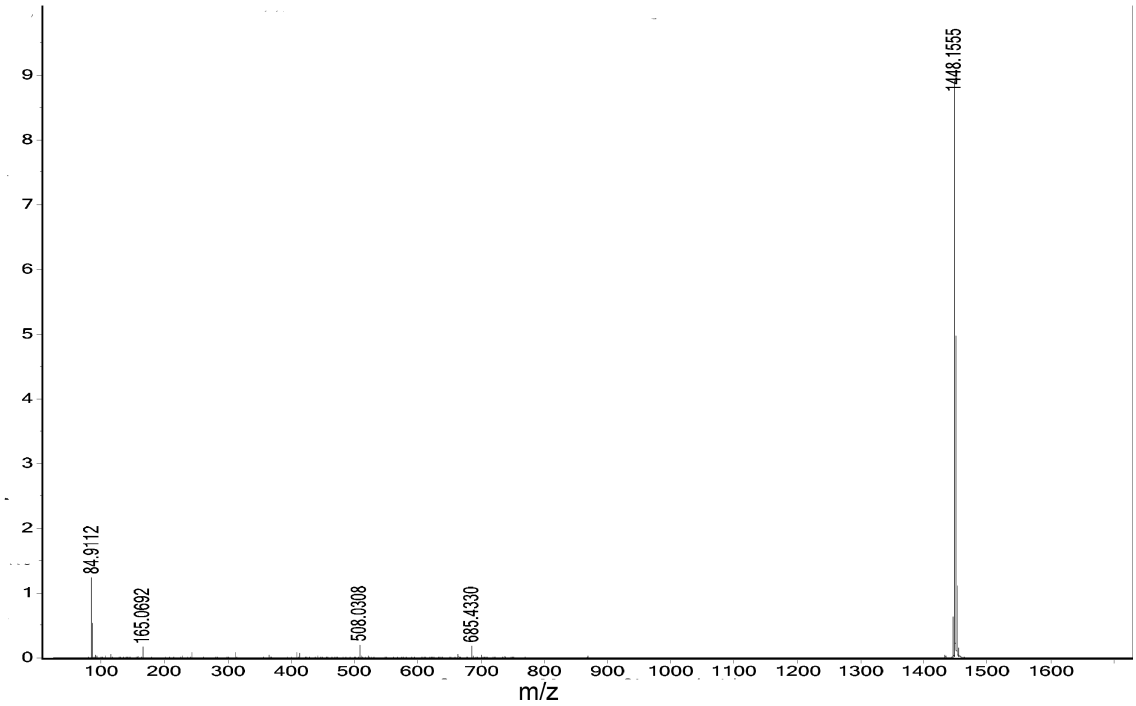

Figure S1.9 High resolution ESI$^+$ mass spectrum of $\{K \subset [In_2(L^{py})_3]\}(PF_6)$

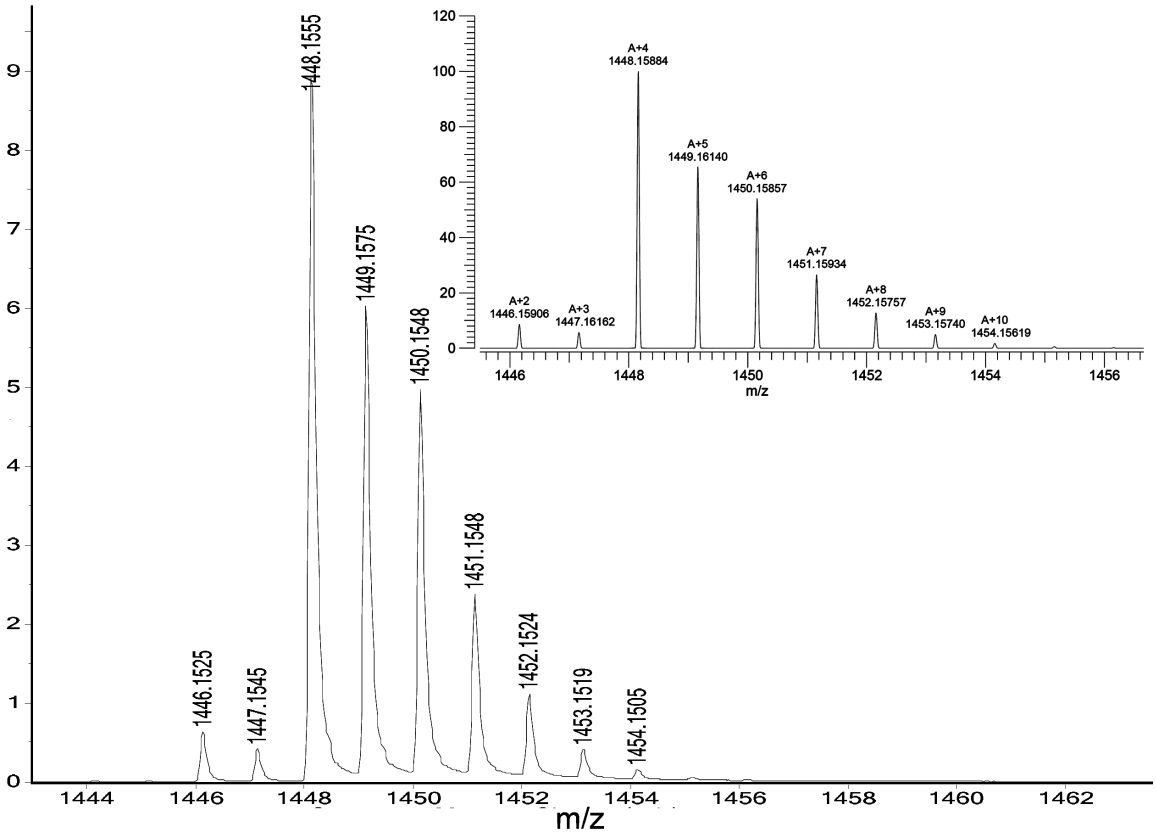

Figure S1.10 Observed and simulated patterns of the based peak in ESI$^+$ mass spectrum of $\{K \subset [In_2(L^{py})_3]\}(PF_6)$

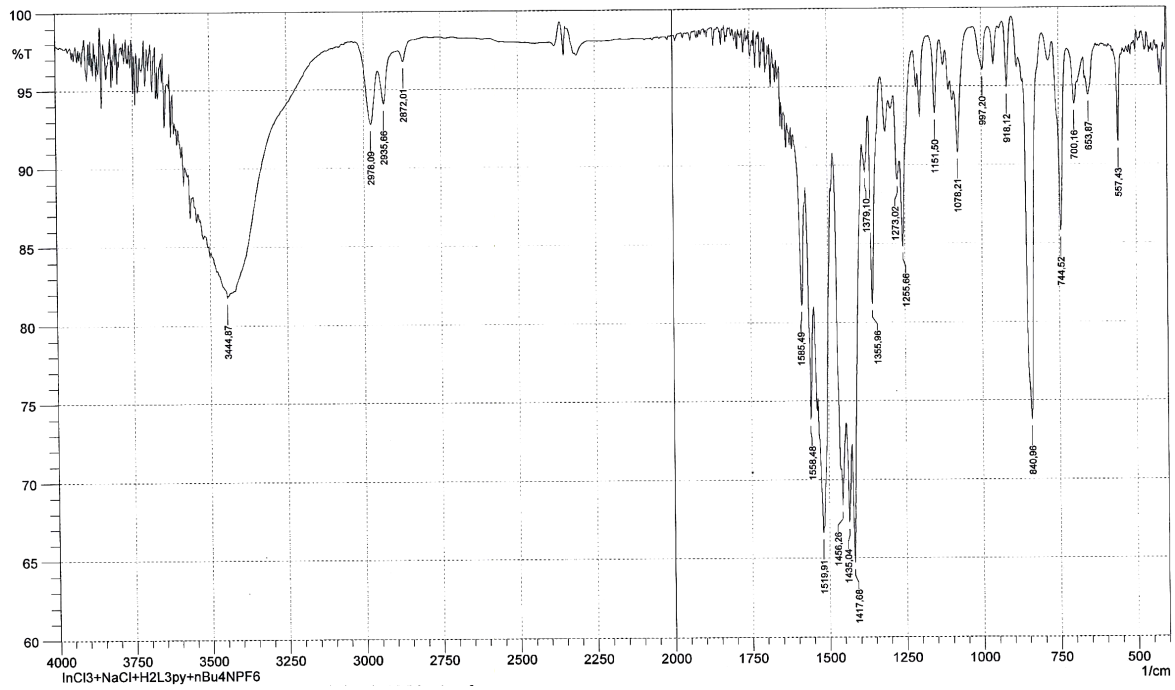

Figure S1.11 IR spectrum of $\{Na \subset [In_2(L^{py})_3]\}(PF_6)$

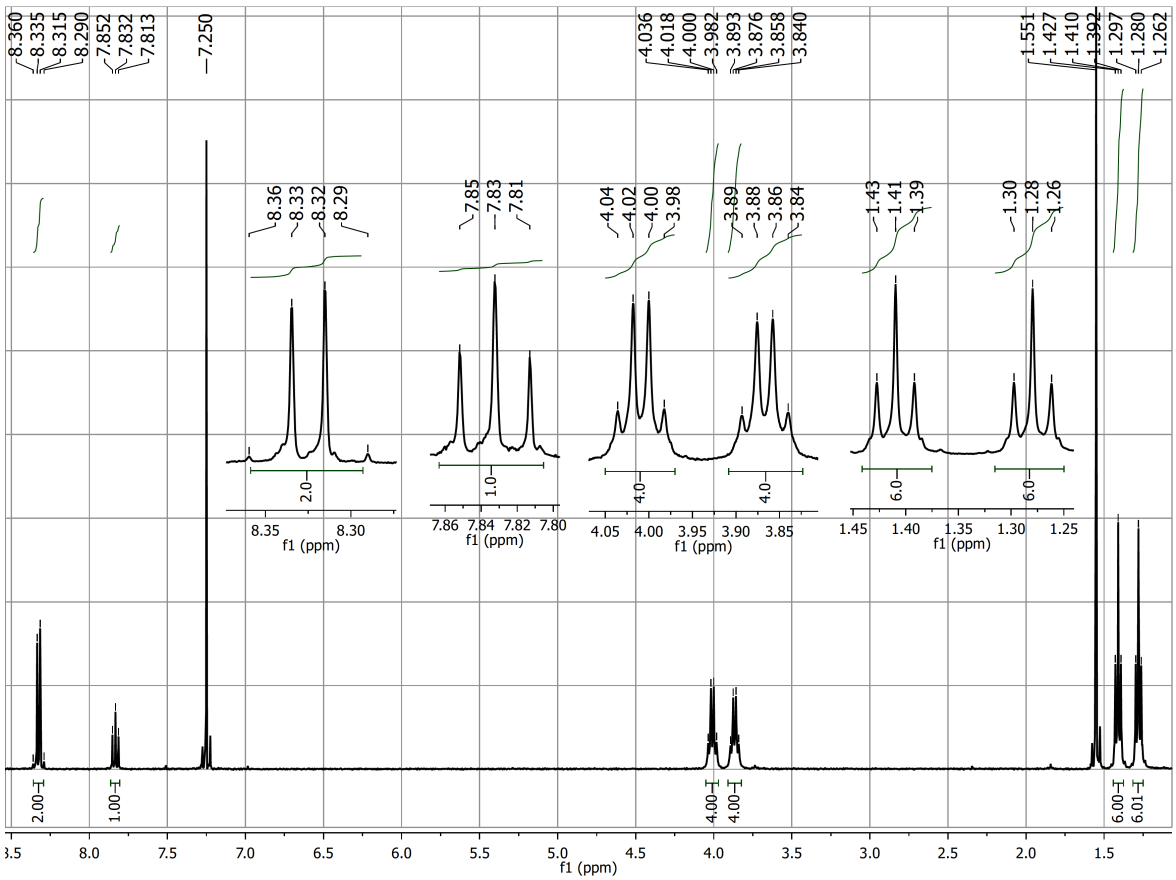

Figure S1.12 ^{1}H NMR spectrum of $\{Na \subset [In_2(L^{py})_3]\}(PF_6)$ in $CDCl_3$

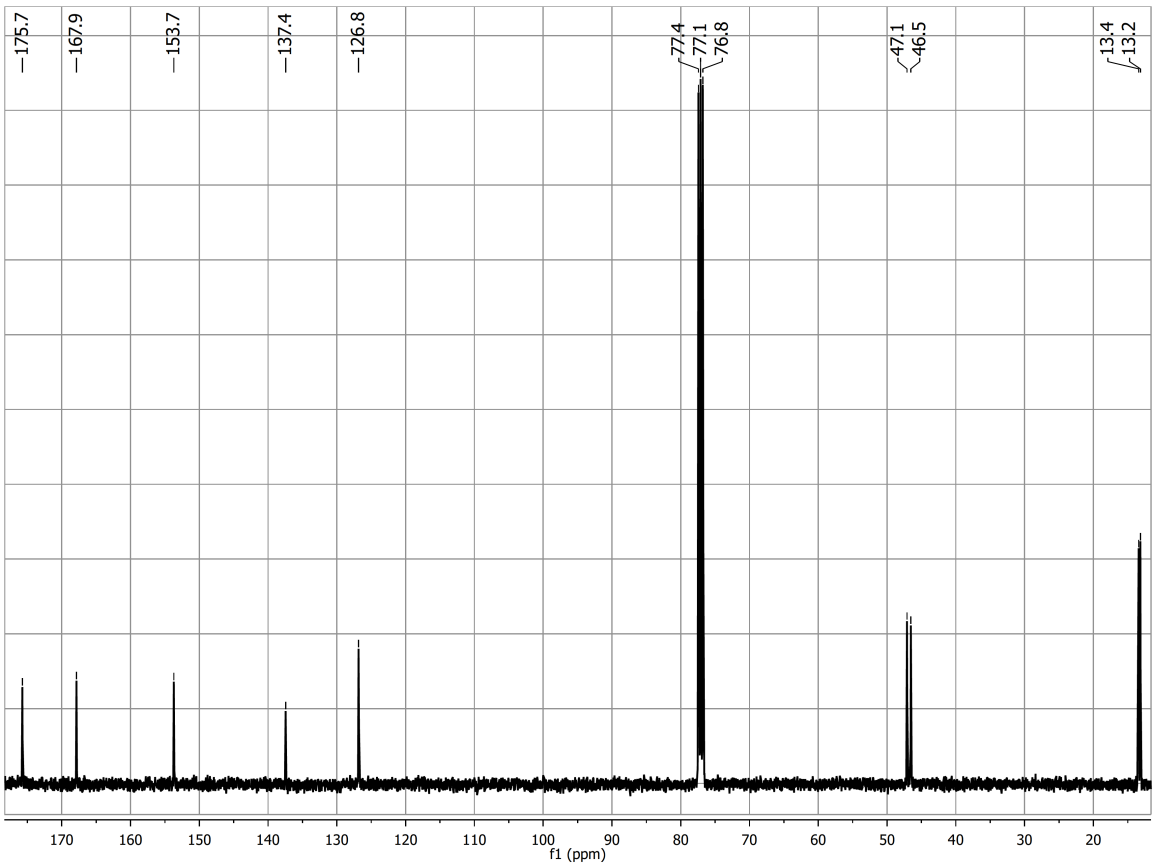

Figure S1.13 $^{13}C\{^{1}H\}$ NMR spectrum of $\{Na \subset [In_2(L^{py})_3]\}(PF_6)$ in $CDCl_3$

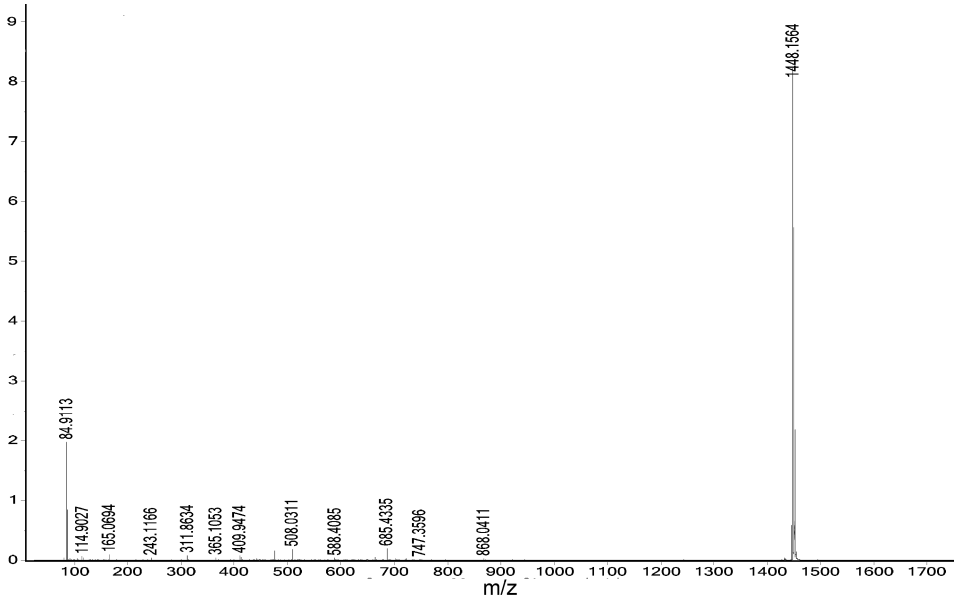

Figure S1.14 High resolution ESI^+ mass spectrum of $\{Na \subset [In_2(L^{py})_3]\}(PF_6)$. The peak of the K^+ inclusion compound is due to interactions with the matrix of the spectrometer, where these ions are present as contaminations.

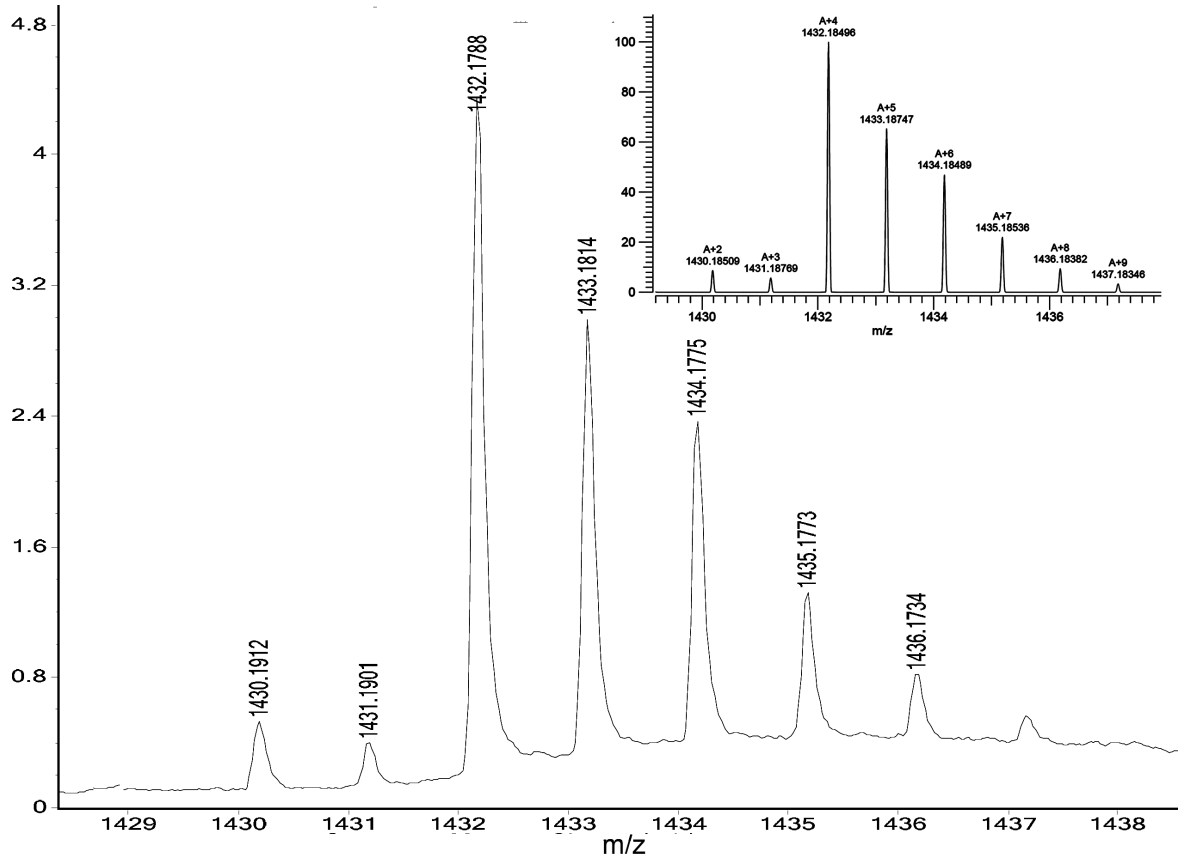

Figure S1.15 Observed and simulated patterns of the molecular peak in ESI$^+$ mass spectrum of $\{Na \subset [In_2(L^{py})_3]\}(PF_6)$

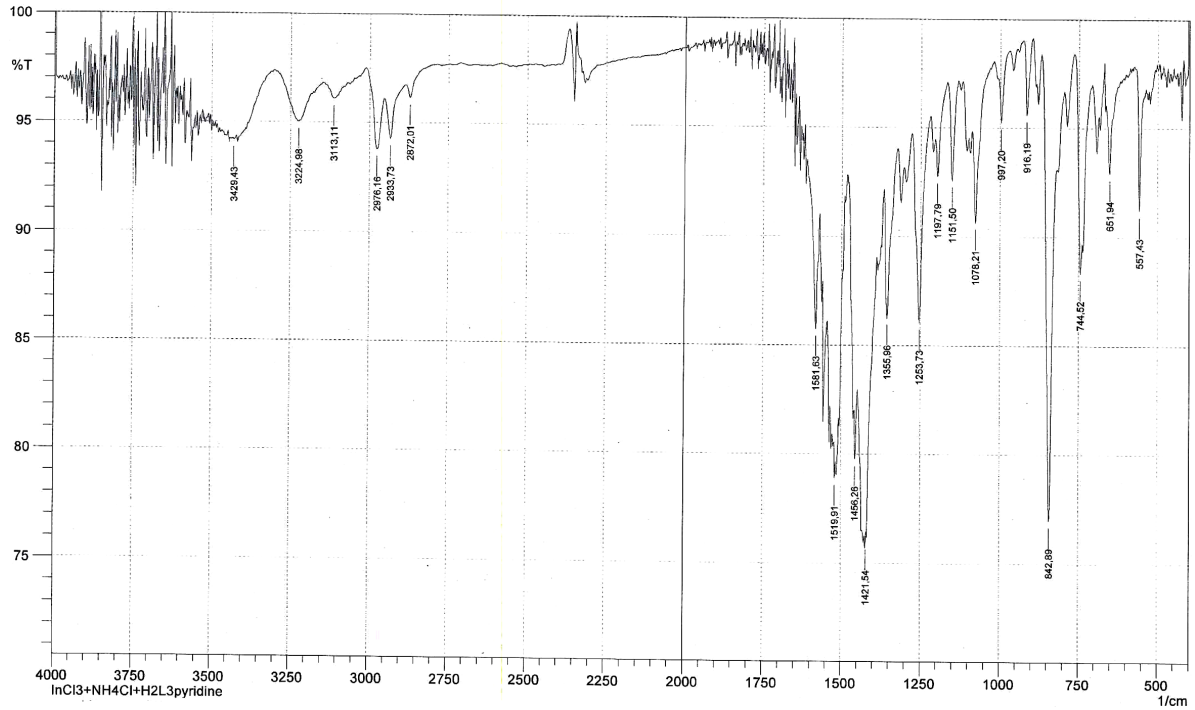

Figure S1.16 IR spectrum of $\{NH_4 \subset [In_2(L^{py})_3]\}(PF_6)$

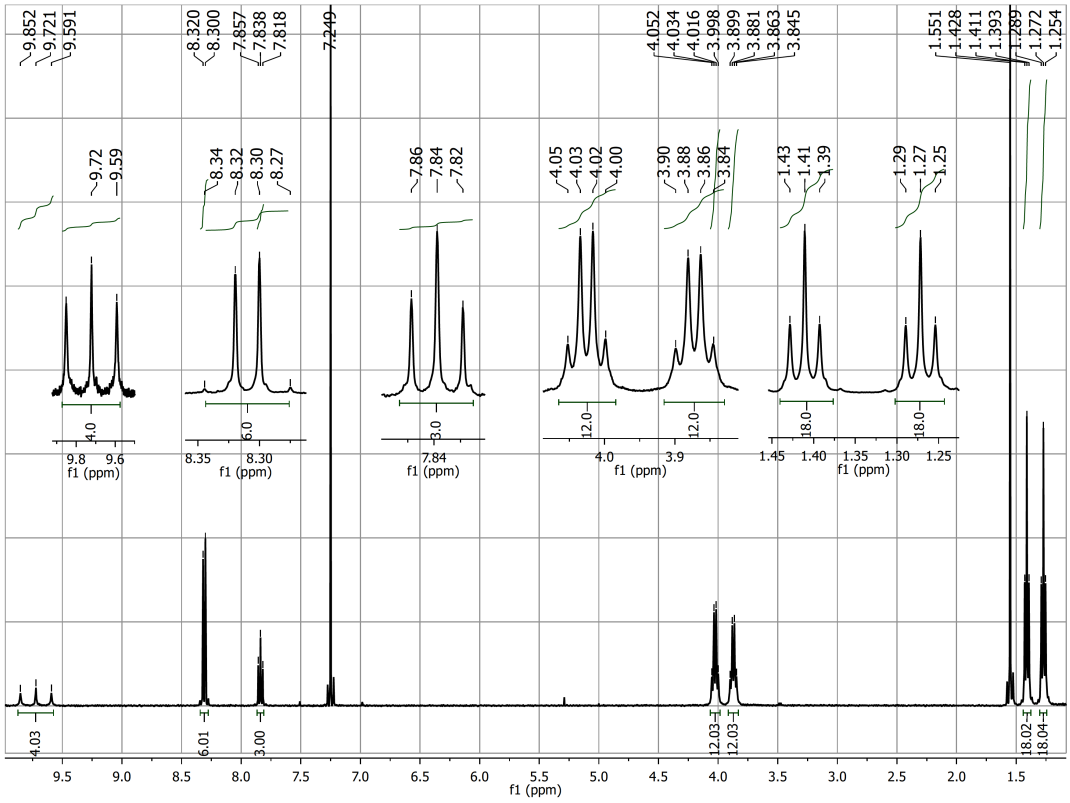

Figure S1.17 ^{1}H NMR spectrum of $\{^{14}NH_4 \subset [In_2(L^{py})_3]\}(PF_6)$ in $CDCl_3$

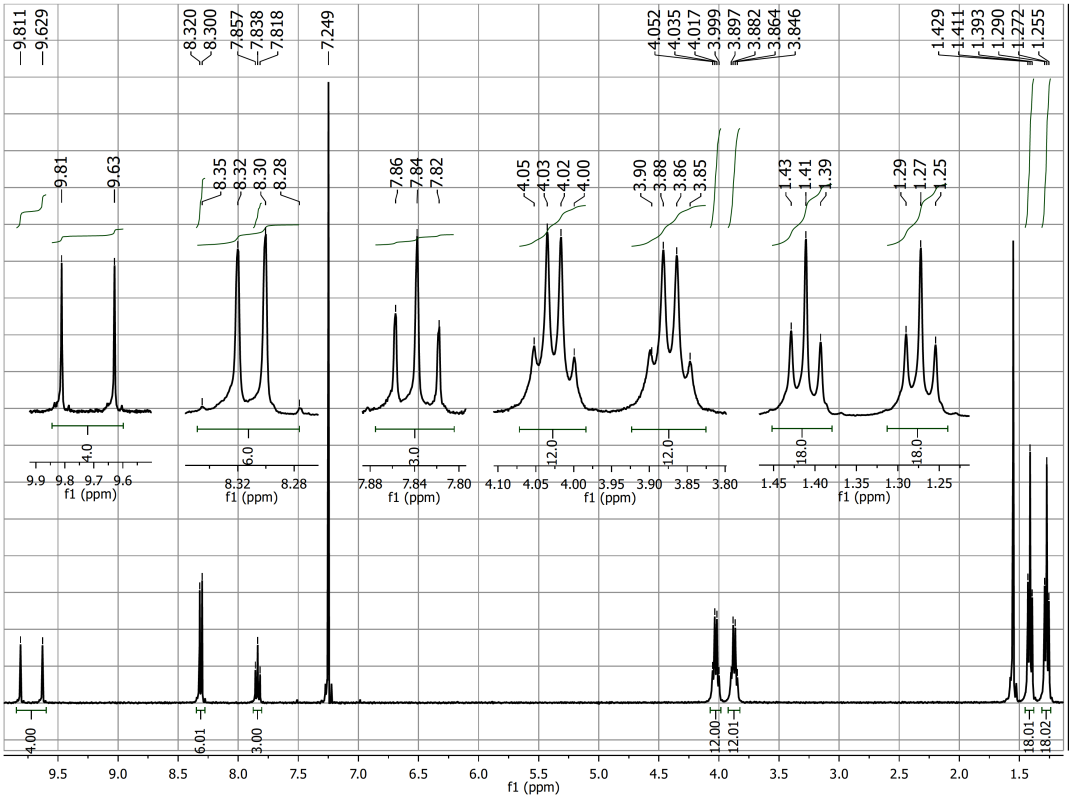

Figure S1.18 ^{1}H NMR spectrum of $\{^{15}NH_4 \subset [In_2(L^{py})_3]\}(PF_6)$ in $CDCl_3$

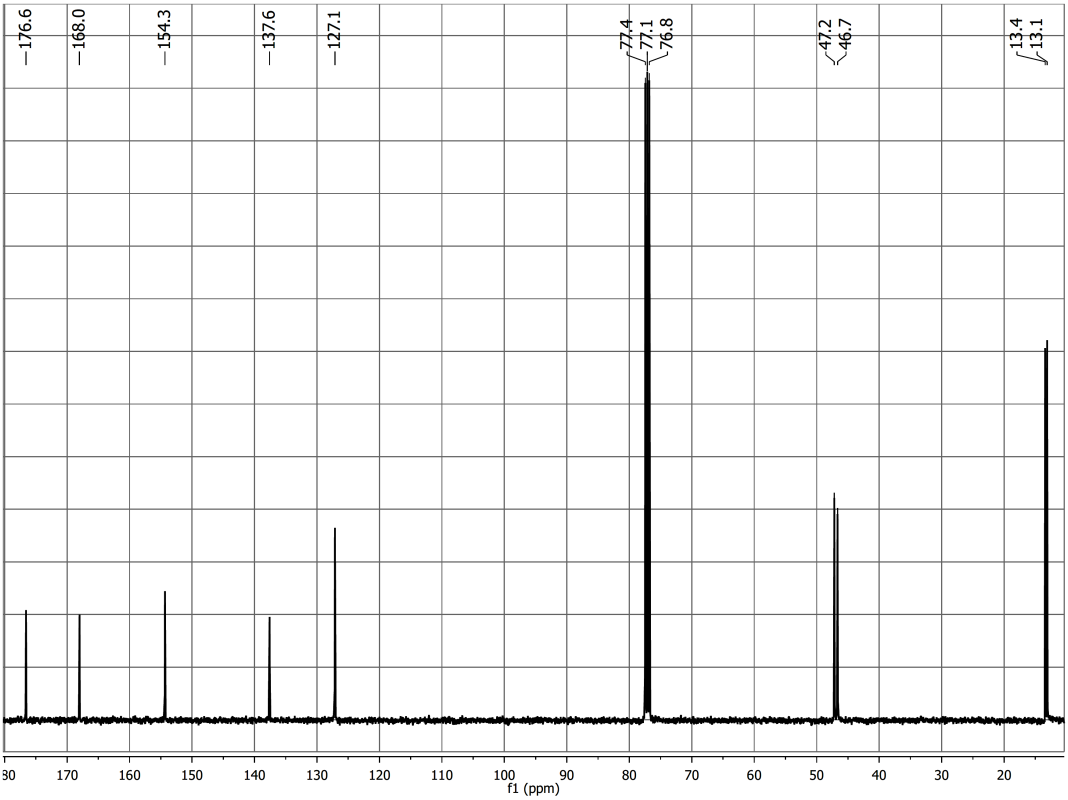

Figure S1.19 ^{13}C{^{1}H} NMR spectrum of $\{NH_4 \subset [In_2(L^{py})_3]\}(PF_6)$ in $CDCl_3$

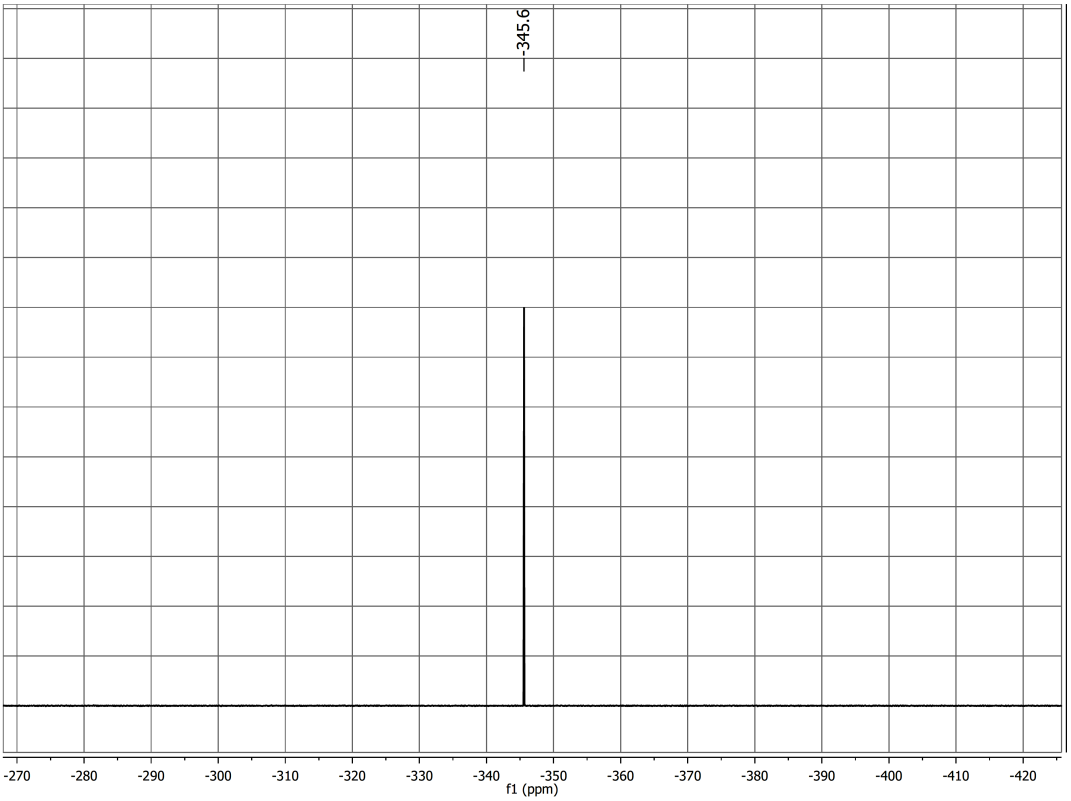

Figure S1.20 $^{15}N\{^{1}H\}$ NMR spectrum of $\{^{15}NH_4 \subset [In_2(L^{py})_3]\}(PF_6)$ in $CDCl_3$

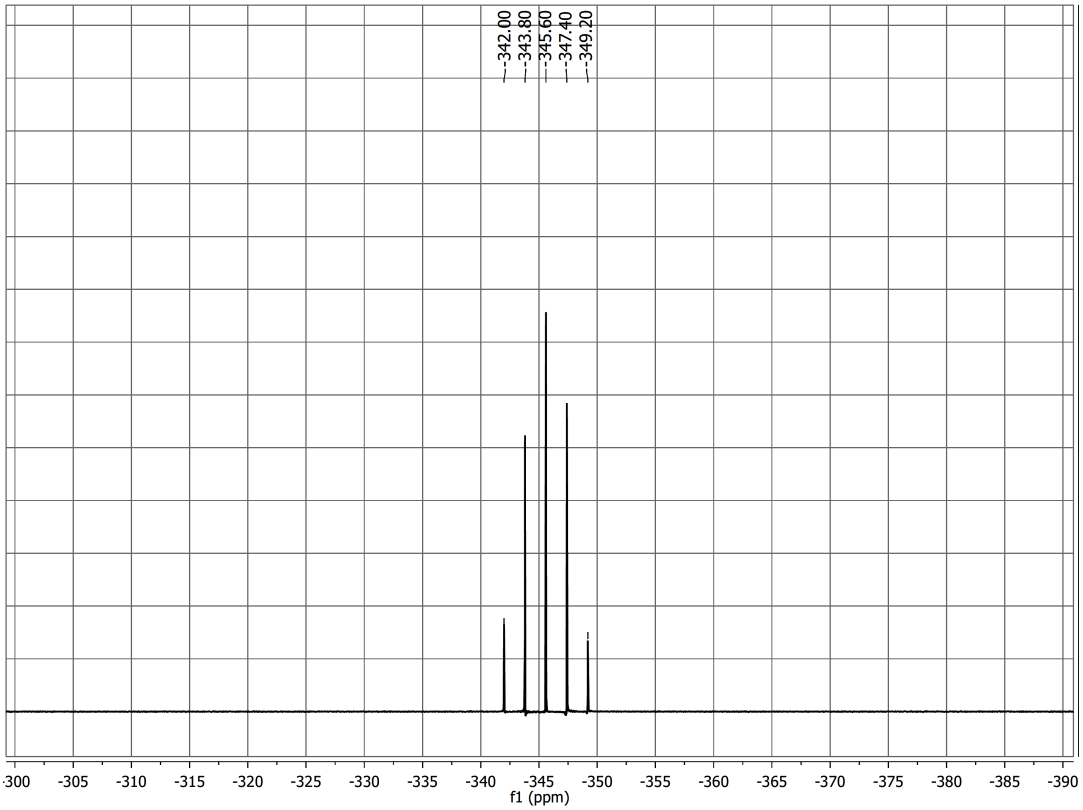

Figure S1.21 ^{15}N DEPT NMR spectrum of $\{^{15}NH_4 \subset [In_2(L^{py})_3]\}(PF_6)$ in $CDCl_3$

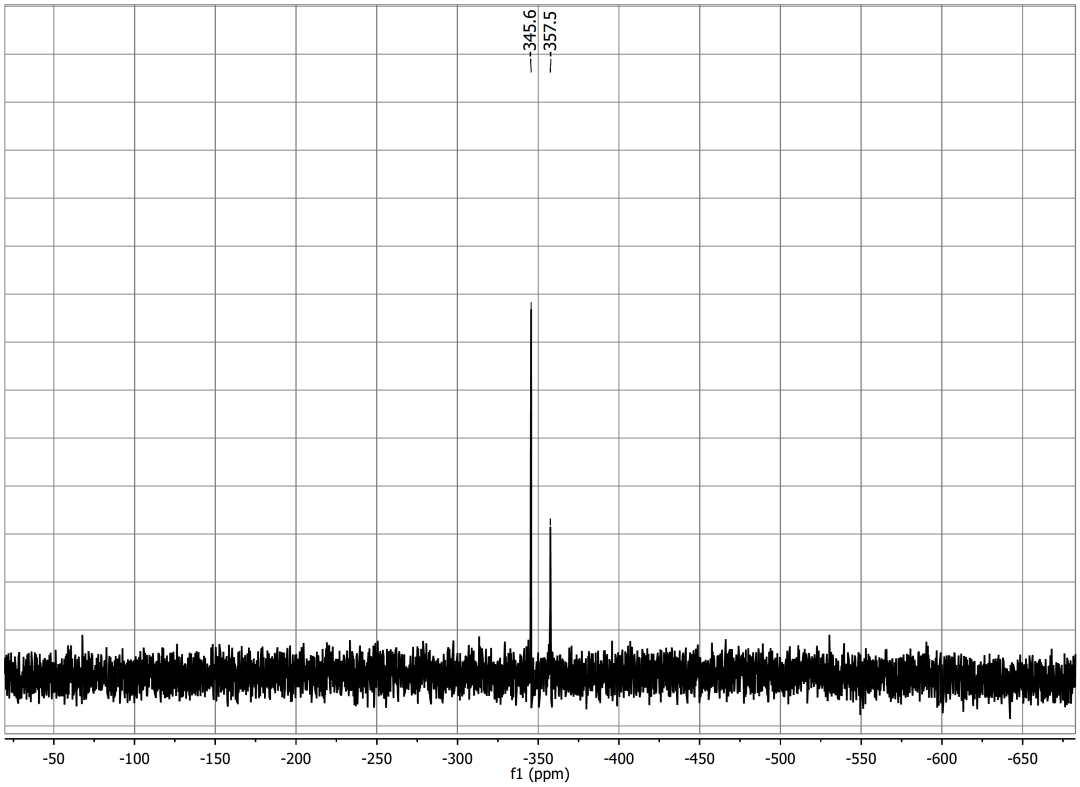

Figure S1.22 $^{15}N\{^{1}H\}$ NMR spectrum of $\{^{15}NH_4 \subset [In_2(L^{py})_3]\}(PF_6)$ in DMSO-d_6

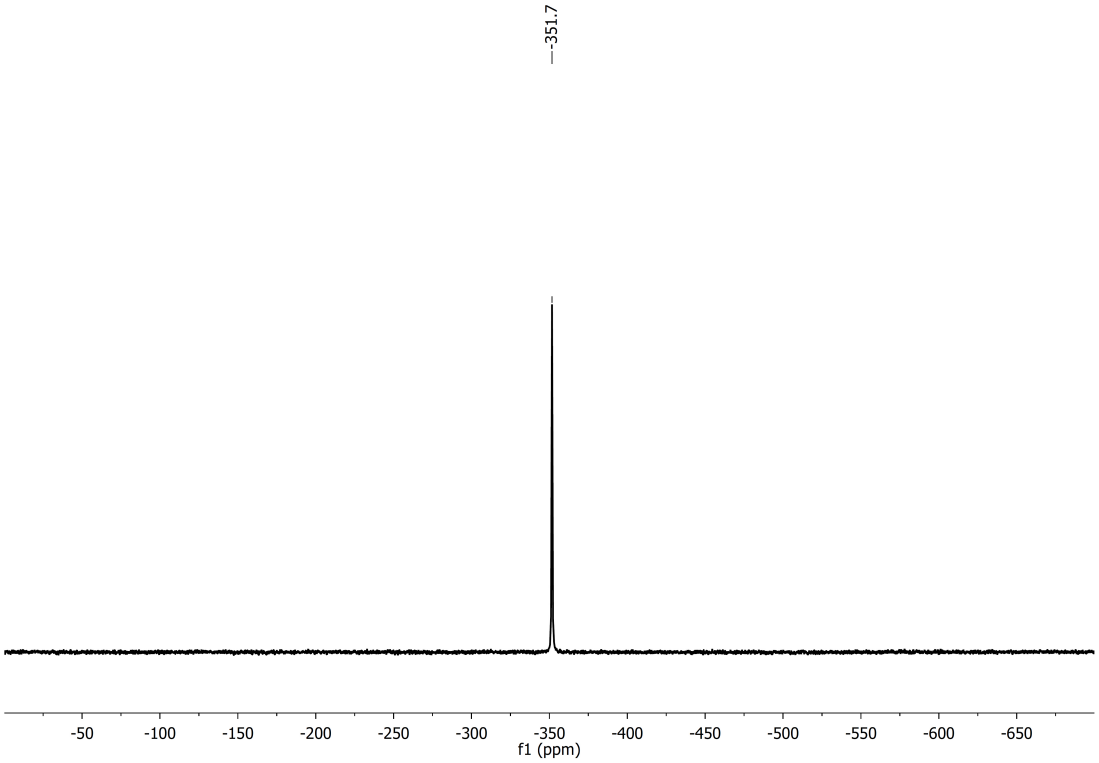

Figure S1.23 $^{15}N\{^{1}H\}$ NMR spectrum of $^{15}NH_4Cl$ in DMSO-d_6

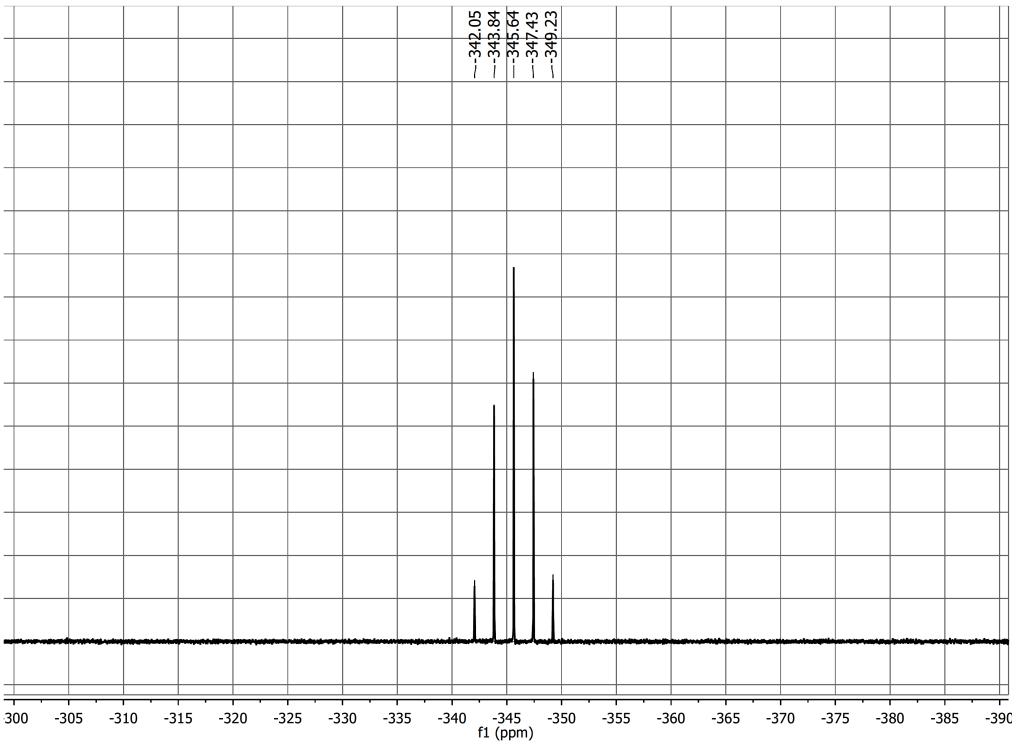

Figure S1.24 ^{15}N DEPT NMR spectrum of $\{^{15}NH_4 \subset [In_2(L^{py})_3]\}(PF_6)$ in DMSO-d_6

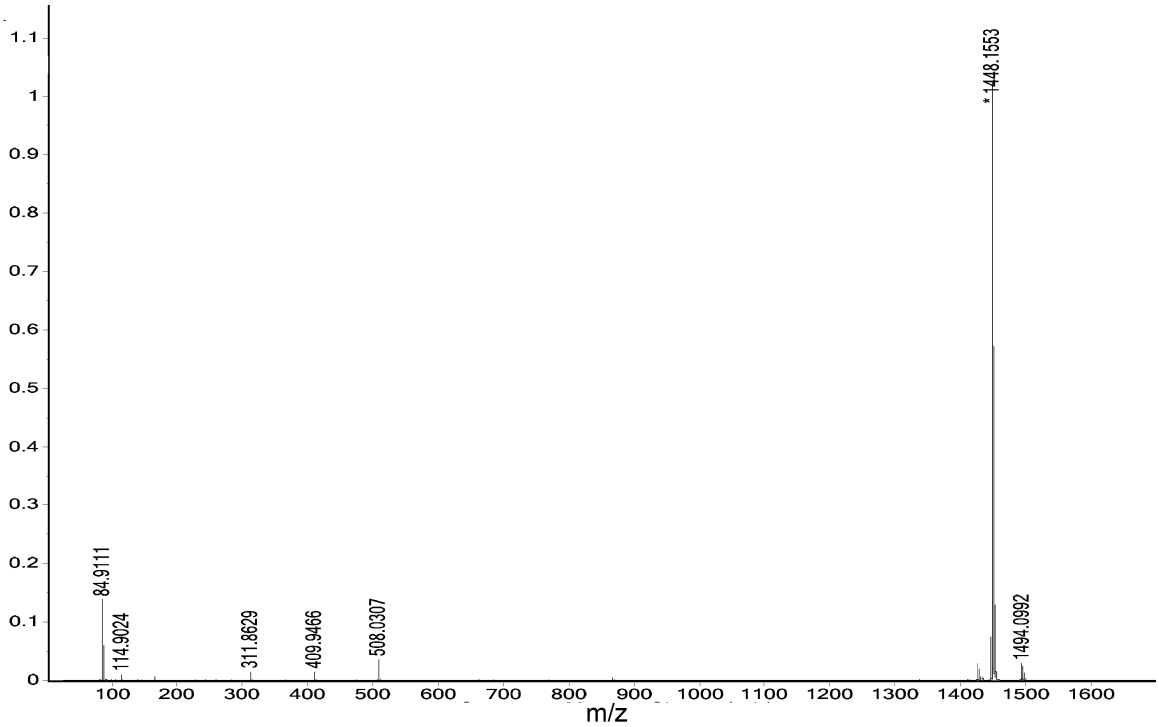

Figure S1.25 High resolution ESI$^+$ mass spectrum of $\{^{14}NH_4 \subset [In_2(L^{py})_3]\}(PF_6)$. The peaks of the K^+ and Rb^+ inclusion compounds are due to interactions with the matrix of the spectrometer, where these ions are present as contaminations.

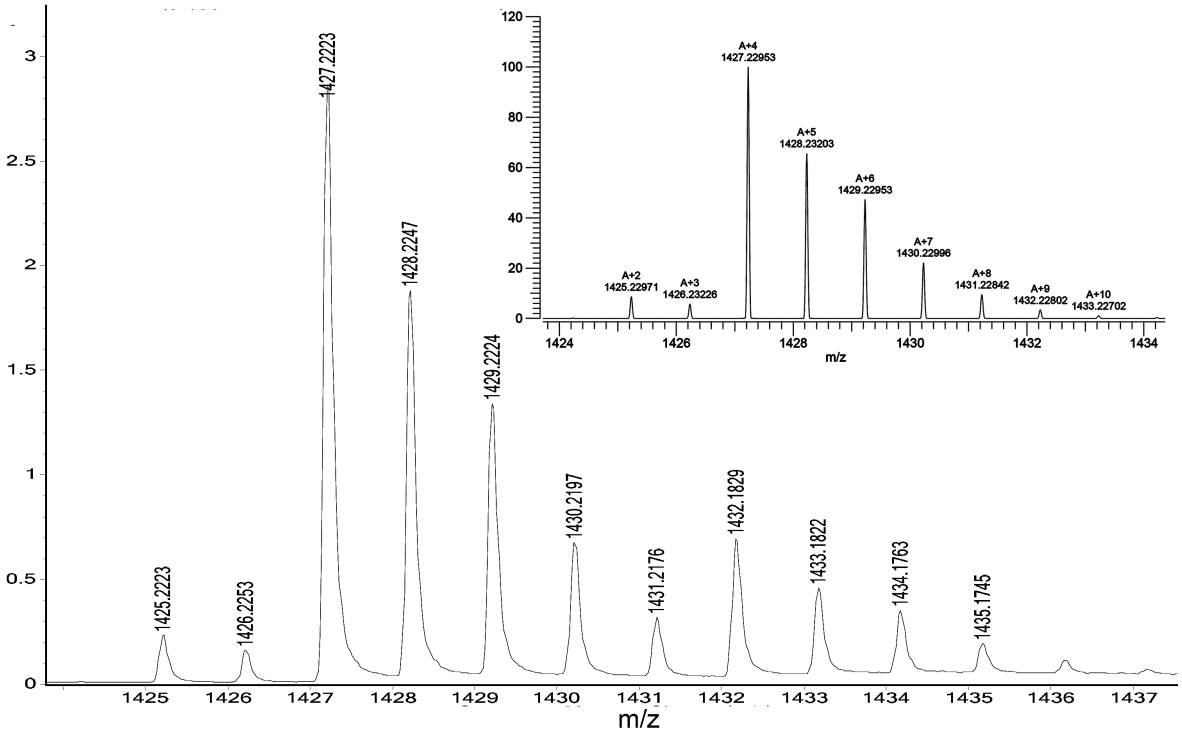

Figure S1.26 Observed and simulated patterns of the molecular peak in ESI$^+$ mass spectrum of $\{^{14}NH_4 \subset [In_2(L^{py})_3]\}(PF_6)$

Part 2 Crystallographic data

Figure S2.1 Ellipsoid representations (50% probability) of H_2L^{py}.

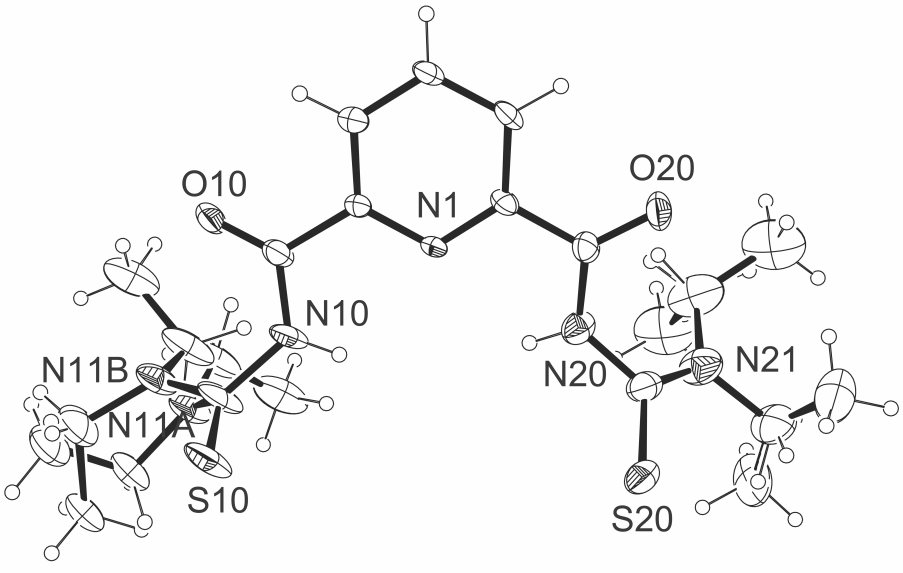

Table S2.1 Hydrogen bonds for H_2L^{py} [Å and °].

D-H...A	d(D-H)	d(H...A)	d(D...A)	<(DHA)
N20-H20...O20$^{\#1}$	0.86	2.54	3.242(16)	139.2
N10-H10...O20$^{\#1}$	0.86	2.15	2.902(16)	146.6

Symmetry transformations used to generate equivalent atoms: $^{\#1}$ x+1/4, -y+5/4, z+1/4.

Figure S2.2 Ellipsoid representations (50% probability) of {Rb ⊂ [$In_2(L^{py}{}_3)$]} (PF_6) · toluene. Hydrogen atoms are omitted for clarity.

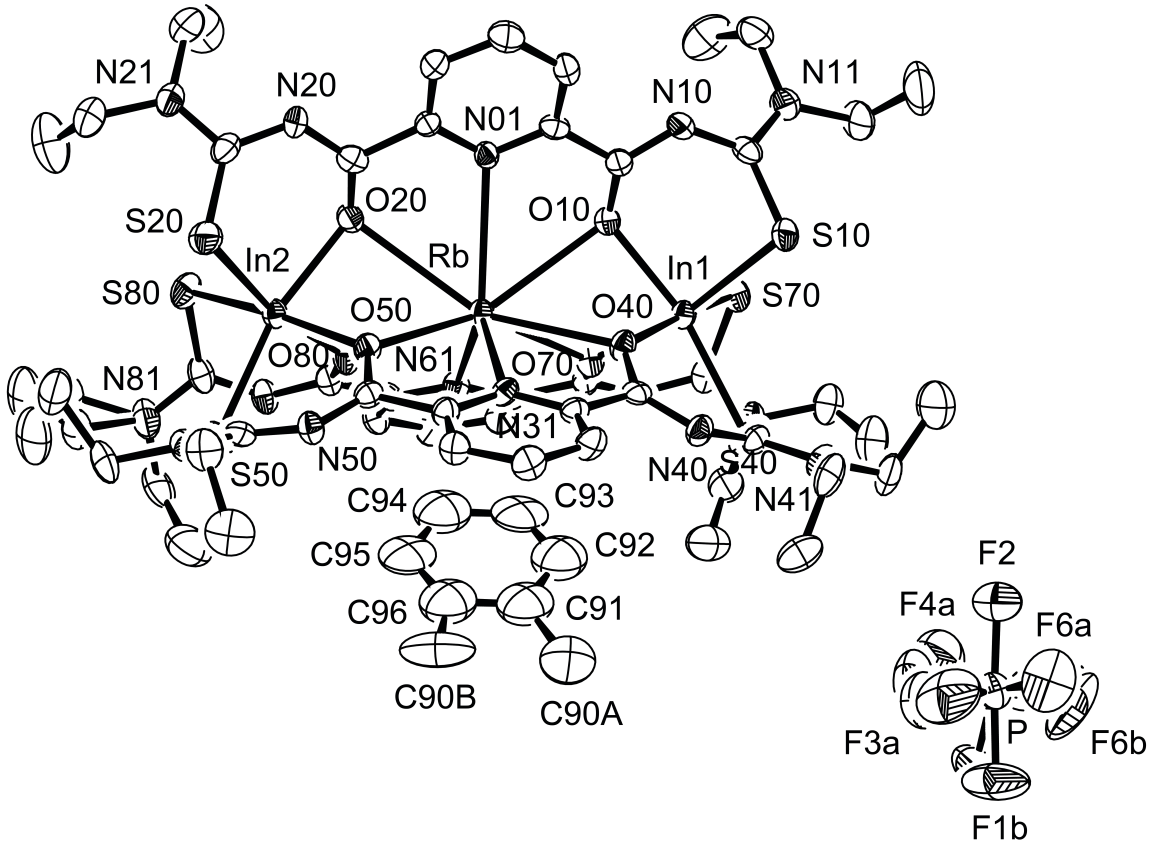

Table S2.2 Selected bond lengths, distances (Å) and bond angles (°) in {Rb ⊂ [$In_2(L^{py}{}_3)$]} (PF_6) · toluene.

Bond lengths, distances (Å)							
In1-O10	2.206(4)	In1-S10	2.5491(15)	Rb-O10	2.898(3)	Rb-N01	2.940(4)
In1-O40	2.192(3)	In1-S40	2.5410(16)	Rb-O20	2.953(3)	Rb-N31	2.983(4)
In1-O70	2.189(4)	In1-S70	2.5427(14)	Rb-O40	2.850(3)	Rb-N61	3.006(5)
In2-O20	2.213(4)	In2-S20	2.5340(15)	Rb-O50	2.823(3)	In1···Rb	3.7477(6)
In2-O50	2.194(3)	In2-S50	2.5487(15)	Rb-O70	2.796(3)	In2···Rb	3.7712(6)
In2-O80	2.182(3)	In2-S80	2.5300(15)	Rb- O80	2.776(4)	In1···In2	7.5189(9)
C10-O10	1.270(6)		C40-O40	1.264(6)		C70-O70	1.281(6)
C10-N10	1.305(6)		C40-N40	1.328(7)		C70-N70	1.301(6)
C11-N10	1.352(6)		C41-N40	1.342(6)		C71-N70	1.354(7)
C11-S10	1.748(6)		C41-S40	1.731(6)		C71-S70	1.742(6)

C20-O20	1.260(6)	C50-O50	1.257(6)	C80-O80	1.258(7)
C20-N20	1.314(6)	C50-N50	1.323(6)	C80-N80	1.317(7)
C21-N20	1.335(7)	C51-N50	1.345(7)	C81-N80	1.336(7)
C21-S20	1.751(6)	C51-S50	1.746(6)	C81-S80	1.752(6)
Bond angles (^{o})					
O10-In1-S40	162.02(10)	O40-In1-S70	170.28(10)	O70-In1-S10	168.04(10)
O10-In1-S10	88.67(10)	O40-In1-S40	83.42(10)	O70-In1-S70	85.45(9)
O20-In2-S50	163.21(11)	O50-In2-S80	167.40(10)	O80-In2-S20	168.46(11)
O20-In2-S20	87.58(10)	O50-In2-S50	83.65(10)	O80-In2-S80	84.85(10)

Figure S2.3 Ellipsoid representations (50% probability) of $\{K \subset [In_2(L^{py}{}_3]\}$ (PF_6) · toluene. Hydrogen atoms are omitted for clarity.

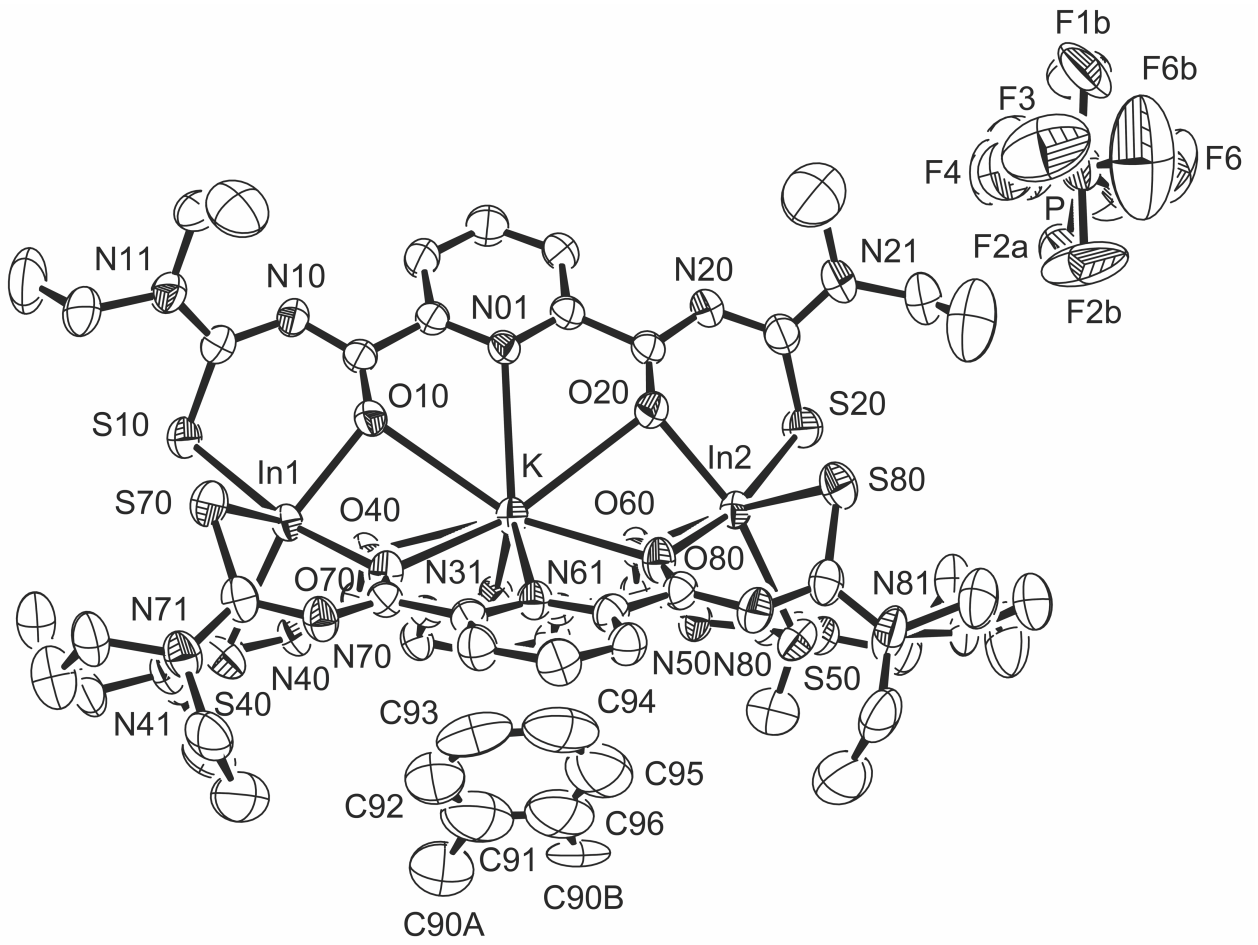

Table S2.3 Selected bond lengths, distances (Å) and bond angles (°) in $\{K \subset [In_2(L^{py}{}_3]\}$ (PF_6) · toluene.

Bond lengths, distances (Å)							
In1-O10	2.208(2)	In1-S10	2.5442(10)	K-O10	2.877(2)	K-N01	2.906(3)
In1-O40	2.187(2)	In1-S40	2.5414(11)	K-O20	2.932(2)	K-N31	2.959(3)
In1-O70	2.174(2)	In1-S70	2.5369(10)	K-O40	2.812(2)	K-N61	2.969 (3)
In2-O20	2.202(2)	In2-S20	2.5343(11)	K-O50	2.783(2)	In1···K	3.7485(8)
In2-O50	2.181(2)	In2-S50	2.5514(10)	K-O70	2.772(2)	In2···K	3.7647(8)
In2-O80	2.177(3)	In2-S80	2.5280(10)	K-O80	2.737(2)	In1···In2	7.5131(9)
C10-O10	1.265(4)		C40-O40	1.274(4)		C70-O71	1.271(4)
C10-N10	1.313(4)		C40-N40	1.318(4)		C70-N70	1.305(4)

C11-N10	1.355(4)	C41-N40	1.347(5)	C71-N70	1.352(4)
C11-S10	1.741(4)	C41-S40	1.741(4)	C71-S70	1.747(4)
C20-O20	1.274(4)	C50-O50	1.259(4)	C80-O80	1.268(4)
C20-N20	1.309(5)	C50-N50	1.322(4)	C80-N80	1.315(4)
C21-N20	1.352(5)	C51-N50	1.344(4)	C81-N80	1.348(5)
C21-S20	1.742(4)	C51-S50	1.742(4)	C81-S80	1.739(4)
Bond angles (^{o})					
O10-In1-S40	161.39(7)	O40-In1-S70	169.06(7)	O70-In1-S10	167.94(7)
O10-In1-S10	88.97(7)	O40-In1-S40	83.40(7)	O70-In1-S70	86.04(7)
O20-In2-S50	162.67(7)	O50-In2-S80	166.43(8)	O80-In2-S20	167.53(7)
O20-In2-S20	88.04(7)	O50-In2-S50	83.76(7)	O80-In2-S80	85.37(7)

Figure S2.4 Ellipsoid representations (50% probability) of $\{NH_4 \subset [In_2(L^{py}{}_3]\}$ (PF_6) · toluene. Hydrogen atoms except those of the ammonium ion have been omitted for clarity.

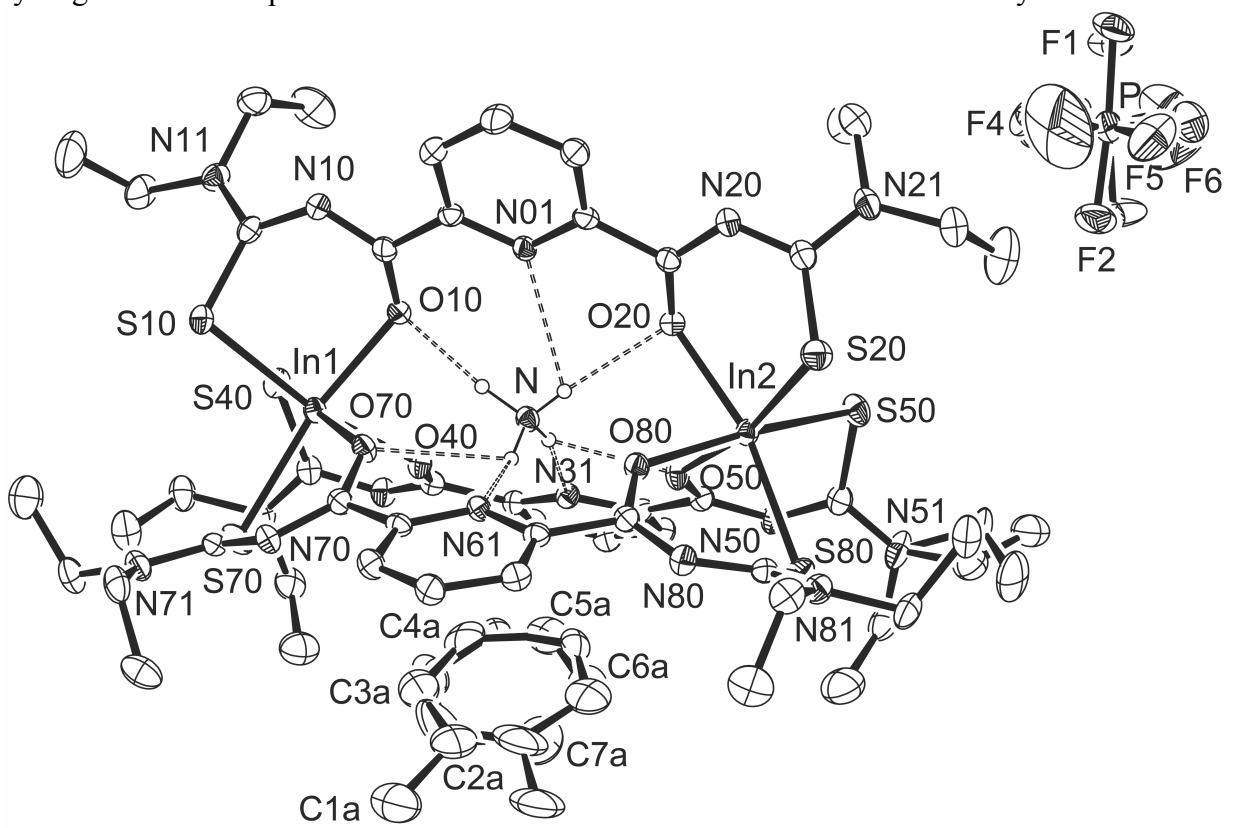

Table S2.4 Selected bond lengths, distances (Å) and bond angles (°) in $\{NH_4 \subset [In_2(L^{py}{}_3]\}$ (PF_6) · toluene.

Bond lengths, distances (Å)					
In1-O10	2.209(2)	In1-O40	2.186(2)	In1-O70	2.195(2)
In1-S10	2.5519(9)	In1-S40	2.5442(9)	In1-S70	2.5399(10)
In2-O20	2.213(2)	In2-O50	2.186(2)	In2-O80	2.184(2)
In2-S20	2.5363(10)	In2-S50	2.5320(8)	In2-S80	2.5515(10)
C10-O10	1.275(4)	C40-O40	1.273(4)	C70-O71	1.263(4)
C10-N10	1.312(4)	C40-N40	1.298(4)	C70-N70	1.320(4)
C11-N10	1.351(4)	C41-N40	1.357(4)	C71-N70	1.335(4)
C11-S10	1.742(4)	C41-S40	1.746(4)	C71-S70	1.749(4)
C20-O20	1.270(4)	C50-O50	1.263(4)	C80-O80	1.257(4)
C20-N20	1.313(4)	C50-N50	1.312(4)	C80-N80	1.320(4)
C21-N20	1.352(4)	C51-N50	1.342(5)	C81-N80	1.349(4)

C21-S20	1.738(4)	C51-S50	1.750(4)	C81-S80	1.750(4)
Bond angles (°)					
O10-In1-S70	162.81(6)	O40-In1-S10	168.18(7)	O70-In1-S40	170.68(6)
O10-In1-S10	88.39(6)	O40-In1-S40	85.31(6)	O70-In1-S70	83.71(6)
O20-In2-S80	163.93(6)	O50-In2-S20	168.65(7)	O80-In2-S50	167.59(7)
O20-In2-S20	87.52(6)	O50-In2-S50	84.79(6)	O80-In2-S80	83.96(6)

Table S2.5 Hydrogen bonds for $\{NH_4 \subset [In_2(L^{py}{}_3]\}(PF_6) \cdot$ toluene [Å and °].

D-H...A	d(D-H)	d(H...A)	d(D...A)	<(DHA)
N-HC...N61	0.85	2.26	3.005(4)	146.4
N-HC...O70	0.85	2.46	2.867(3)	110.3
N-HB...N31	0.85	2.18	3.002(4)	164.1
N-HB...O50	0.85	2.25	2.784(3)	121.4
N-HD...O10	0.98(4)	1.92(4)	2.891(4)	173(3)
N-HA...N01	0.80(4)	2.50(4)	2.915(4)	114(3)
N-HA...O20	0.80(4)	2.15(4)	2.945(3)	172(4)